

THE GALAXY EVOLUTION EXPLORER A SPACE ULTRAVIOLET SURVEY MISSION

D. CHRISTOPHER MARTIN¹, JAMES FANSON¹⁰, DAVID SCHIMINOVICH¹, PATRICK MORRISSEY¹, PETER G. FRIEDMAN¹,
TOM A. BARLOW¹, TIM CONROW¹, ROBERT GRANGE³, PATRICK N. JELINSKY⁵, BRUNO MILLIARD³, OSWALD H. W.
SIEGMUND⁵, LUCIANA BIANCHI⁴, YONG-IK BYUN², JOSE DONAS³, KARL FORSTER¹, TIMOTHY M. HECKMAN⁴, YOUNG-WOOK
LEE², BARRY F. MADORE^{6,7}, ROGER F. MALINA³, SUSAN G. NEFF⁸, R. MICHAEL RICH⁹, TODD SMALL¹, ALEX S. SZALAY⁴
AND TED K. WYDER¹

Submitted to Ap.J.Letters

ABSTRACT

We give an overview of the Galaxy Evolution Explorer (GALEX), a NASA Explorer Mission launched on April 28, 2003. GALEX is performing the first space UV sky-survey, including imaging and grism surveys in two bands (1350-1750Å and 1750-2750Å). The surveys include an all-sky imaging survey ($m_{AB} \simeq 20.5$), a medium imaging survey of 1000 deg² ($m_{AB} \simeq 23$), a deep imaging survey of 100 square degrees ($m_{AB} \simeq 25$), and a nearby galaxy survey. Spectroscopic grism surveys ($R=100-200$) are underway with various depths and sky coverage. Many targets overlap existing or planned surveys. We will use the measured UV properties of local galaxies, along with corollary observations, to calibrate the UV-global star formation rate relationship in local galaxies. We will apply this calibration to distant galaxies discovered in the deep imaging and spectroscopic surveys to map the history of star formation in the universe over the redshift range $0 < z < 1.5$, and probe the physical drivers of star formation in galaxies. The GALEX mission includes a Guest Investigator program supporting the wide variety of programs made possible by the first UV sky survey.

Subject headings: space missions; UV astrophysics; galaxy evolution; surveys

1. MOTIVATION FOR GALEX

The Galaxy Evolution Explorer (GALEX), a NASA Small Explorer mission, is performing the first all-sky, deep imaging and spectroscopic surveys in the space ultraviolet (1350-2750Å). The prime goal of GALEX is to study star formation in galaxies and its evolution with time. GALEX primary mission surveys and dedicated observations for the Guest Investigator Program, beginning October 2004, will also support a broad array of other investigations.

1.1. *Galaxy Evolution*

Tinsley, in her seminal 1968 paper (Tinsley 1968), demonstrated that passive stellar evolution and an evolving stellar birthrate required to match the properties of nearby galaxies had a profound impact on the appearance of galaxies observed over cosmological distances. It

is now doctrine that galaxies cannot be used as standard candles for cosmological tests. The study of distant galaxies has become an exploration of the physical processes that assembled luminous matter in the cores of growing dark matter halos.

Tinsley observed that the diversity of galaxies we see today is at its core a diversity in star formation histories. A central goal of cosmology is to measure and explain the star formation, gas depletion, and chemical evolution history in galaxies. Two major developments in the mid 1990's led new urgency to this goal. The first was the discovery of a population of star-forming Lyman Break galaxies (LBGs) at $z \sim 3$ (Steidel et al. 1996). The second was the prediction (Fall, Charlot, & Pei 1996), based on QSO absorption line evolution, and first evidence (Lilly, Le Fevre, Hammer, & Crampton 1996) for strong evolution in the total cosmic star formation rate. These culminated in the now famous plot (Madau et al. 1996) of cosmic star formation history, which hinted that SFR density in the universe was a ten times more vigorous and peaked 5-8 Gyrs ago. A major goal is to delineate the cosmic star formation history using any and all metrics. In part because of the diversity of techniques the current plot remains a weak constraint on cosmogenic models. A parallel effort is now underway to measure the cosmic stellar mass history (Dickinson, Papovich, Ferguson, & Budavári 2003)– if the stellar initial mass function is universal and constant, these histories must agree.

The rest UV provides a powerful tool for measuring and understanding star formation in galaxies at all epochs, a fact underscored by the discovery and study of Lyman Break Galaxies. As emphasized by Adelberger and Steidel (2000), even when dust extinction is very large, rest UV luminosities remain large enough to be detected in UV-selected surveys. JWST will extend rest

¹ California Institute of Technology, MS 405-47, 1200 East California Boulevard, Pasadena, CA 91125

² Center for Space Astrophysics, Yonsei University, Seoul 120-749, Korea

³ Laboratoire d'Astrophysique de Marseille, BP 8, Traverse du Siphon, 13376 Marseille Cedex 12, France

⁴ Department of Physics and Astronomy, The Johns Hopkins University, Homewood Campus, Baltimore, MD 21218

⁵ Space Sciences Laboratory, University of California at Berkeley, 7 Gauss Way, Berkeley, CA 94720

⁶ Observatories of the Carnegie Institution of Washington, 813 Santa Barbara St., Pasadena, CA 91101

⁷ NASA/IPAC Extragalactic Database, California Institute of Technology, Mail Code 100-22, 770 S. Wilson Ave., Pasadena, CA 91125

⁸ Laboratory for Astronomy and Solar Physics, NASA Goddard Space Flight Center, Greenbelt, MD 20771

⁹ Department of Physics and Astronomy, University of California, Los Angeles, CA 90095

¹⁰ Jet Propulsion Laboratory, California Institute of Technology, 4800 Oak Grove Drive, Pasadena, CA 91109

UV selection to redshifts of 5-20, perhaps the first generation of stars. Ironically, the interpretation of high redshift galaxies in the rest UV is most limited by the lack of large, systematic surveys of low redshift UV galaxies serving as a benchmark.

While the initial conditions that led to structure formation in the Universe are becoming clear (de Bernardis, P. et al. 2000; Bennett et al. 2003), the formation and evolution of galaxies is tied to the complex behavior of gas dissipating and cooling within dark matter halos and feedback from massive stars. Fundamentally lacking in numerical simulations and semi-analytic models is a predictive physical model for star formation.

1.2. The UV Sky – Precursors to GALEX

Technological obstacles have slowed progress in mapping the UV sky to a steady series of important, but incremental advances. The Orbital Astronomical Observatory OAO-2 (Code et al. 1970) provide the first systematic UV photometry and spectrophotometry of bright stars, globular clusters and nearby galaxies. The TD-1 satellite performed an all-sky spectrophotometric survey of objects to a visual magnitude of 9-10 (Boksenberg et al. 1973). The Astronomical Netherlands Satellite (ANS) (van Duinen et al. 1975) made UV observations of stars, globular clusters, planetary nebulae, and galaxies. The highly successful International Ultraviolet Explorer (Kondo 1987), the first satellite mission to use an imaging UV detector, obtained thousands of targeted low and high resolution spectra in the 1200-3000Å band. Along with many other results, these targeted missions provided the foundation for galaxy stellar population synthesis models in the UV.

UV survey experiments, beginning in the 1970's, used intensified film photography and relatively small telescope apertures. Wide field UV surveys were performed aboard Skylab (Henize et al. 1975), by a lunar camera erected by Apollo 16 astronauts (Carruthers 1973), and by the Spacelab FAUST instrument (Bowyer, Sasseen, Lampton, & Wu 1993). The Ultraviolet Imaging Telescope (Stecher et al. 1997) obtained a wealth of UV images and results over two Shuttle Astro missions. The balloon-borne FOCA Telescope (Milliard, Laget, & Donas 1992) obtained the first far UV luminosity function for galaxies in the local universe (Treyer et al. 1998) and the first rest UV anchor point for the star formation history plot.

1.3. GALEX Goals

The GALEX mission was therefore designed with three overarching primary science goals. All three goals require the primary GALEX UV surveys and multiwavelength corollary data. GALEX surveys are therefore designed to exploit existing and planned surveys in other bands.

The first goal is to provide a calibration of UV and galaxy star formation rate, accounting for, in order of declining impact, extinction, starburst history, initial mass function and metallicity. This calibration would be obtained over a wide range of star formation environments and modalities, so that the relationships can be applied to galaxies at cosmic epochs where star formation may assume a very different character. As we show in Figure 1, UV provides a measure of star formation on timescales $\sim 10^8$ yrs. In galaxies with smoothly

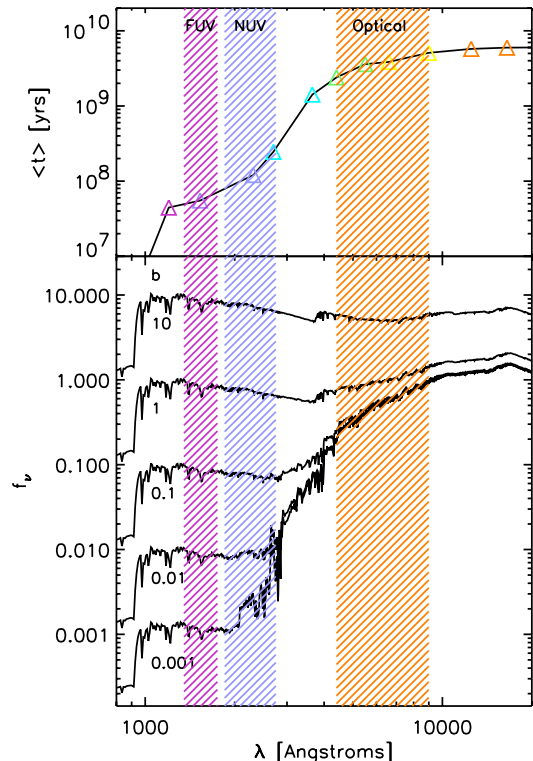


FIG. 1.— TOP: Light-weighted age of a Simple Stellar Population from Bruzual and Charlot (2003), vs. wavelength. UV traces star formation over timescales of $10^{7.5-8.5}$ yrs. BOTTOM: Flux from old plus young stellar population, for values of $b = \dot{M} / \langle \dot{M} \rangle$ ranging from $b=10$ to $b=0.001$.

varying star formation histories, UV provides a linear measure of the current star formation rate once the extinction problem is solved. A major GALEX objective is to determine the minimum set of observations required to measure intrinsic extinction, in the spirit of the starburst UV slope-infrared excess relationship of Meurer, Heckman, & Calzetti (1999). In galaxies with more complex star formation histories, UV probes timescales relevant to starbursts triggered by major interactions and mergers, a core element of hierarchical structure models.

The second GALEX goal is to use the rest UV surveys to determine the cosmic star formation history over the redshift range $0 < z < 1.5$ (the last 9 Gyrs) and its dependence on environment, mass, morphology, merging, and star formation modality (notably quiescent vs. interacting/merging). This history could then be laid side by side with ground, HST, JWST, and other optical-near IR surveys of rest UV galaxies at redshifts $1.5 < z < 20$ (the first 4 Gyrs) to yield a consistent measurement of galaxy building over the age of the universe. A key strength of rest UV observations is the decoupling of recent and old star formation histories. As we show in Figure 1, rest UV scales with star formation rate over a very wide range of specific star formation rates.

Finally, using both the large statistical samples and detailed studies of nearby galaxies, again with abundant multiwavelength data, GALEX will attack the goal of a predictive model of global star formation rates in diverse contexts.

TABLE 1
GALEX ON-ORBIT PERFORMANCE

Effective Area	20-50 cm ²
Angular resolution	4.5-6'' FWHM
Spectral Resolution	100-250
Field of View	1.2 degrees
Bands (simultaneous)	FUV 1350-1750Å; NUV 1750-2750Å
Sensitivity (AB mag)	100 s 20.5 [AIS] 1 ks 23.5 [MIS/NGS] 30 ks 25.5 [DIS]
Astrometry	1 arcsec (rms)
Observations	Nighttime-1 eclipse=1000-2000 s
Mission Length	Baseline 28 months, Minimum 12 months

2. MISSION OVERVIEW

2.1. Observatory Design

The GALEX instrument employs a novel optical design using a 50 cm diameter modified Ritchey-Chrétien telescope with four channels, including FUV and NUV imaging, and FUV and NUV spectroscopy. The telescope has a focal length of 3 meters, and is coated with Al-MgF₂. The field of view is 1.2 degrees circular. Imaging, grism, and opaque modes are selected with an optics wheel with a CaF₂ imaging window, a CaF₂ transmission grism, and an opaque position. Spectroscopic observations are obtained at multiple grism position angles, also selectable, to remove spectrum overlap effects. The FUV (1350-1750Å) and NUV (1750-2750Å) bands are obtained simultaneously using a dichroic beam splitter that also acts as a field aberration corrector. The beam splitter/asphere is an ion-etched fused silica plate with aspheric surfaces on both sides. Beam splitting is accomplished with a dielectric multilayer on the input side which reflects the FUV band and transmits the NUV band. The detectors are sealed tube microchannel plate detectors with 65 mm active area and crossed delay-line anodes for photon event position readout. The far UV detector is preceded by a blue-edge filter which blocks the night-side airglow lines of OI1304, 1356, and Ly α . The near UV detector is preceded by a red block filter/fold mirror, which produces a sharper long-wavelength cut-off than the detector CsTe photocathode and thereby reduces the zodiacal light background and optical contamination. The far UV detector has a MgF₂ window which includes power for field flattening, and an opaque CsI photocathode. The near UV detector has a Fused Silica window which also includes power for field flattening, and a semitransparent Cs₂Te photocathode proximity focused across a 300 μ m gap. The detector peak QE is 12% (FUV) and 8% (NUV). In orbit dark background is low, XXX/XXX cps (FUV/NUV) for diffuse background, as compared to the lowest total night sky backgrounds of 1500/10,000 cps. The detectors are linear up to a local (stellar) countrate of 100 c/s, which corresponds to $m_{AB} \sim 14-15$. The system angular resolution, which includes contributions from the optical and detector PSF, and ex post facto aspect reconstruction, is typically 4.5/6.0 (FUV/NUV) arcseconds (FWHM), and varies by $\sim 20\%$ over the field of view due to variations in the detector resolution, the dominant term. The grism, fabricated by Jobin-Yvon in Paris, is a ruled CaF₂ prism with a small curvature on the input side. In order to

provide simultaneous coverage of the 1350-2750Å range, the grism is blazed in 1st order for the NUV band and in 2nd order for the FUV band, and obtains peak absolute efficiencies of 80% and 60% respectively. Spectral resolution is 200/100 (FUV 2nd order/NUV 1st order). On orbit angular resolution and instrument throughput are as expected from ground calibration. A more complete description of the instrument and satellite can be found in Martin et al. (2003).

2.2. Mission Operations

GALEX was launched by a Pegasus-XL vehicle on April 28, 2003 into a 29 degree inclination, 690 km circular, 98.6 minute orbit. GALEX began nominal operations on August 2. The eight surveys listed in Table 2 are being performed concurrently for the first 38 months. The mission design is simple. Science data is obtained only on the night side. On the day side, the satellite is in solar panel-sun orientation. As the satellite enters twilight, it slews to one of the survey targets. The imaging window or grism is selected, and the detector high voltage ramped from idle. All observations are performed in a pointed mode with an arcminute spiral dither to average non-uniformities and to prevent detector fatigue by bright stars. Individual photon events, time-tagged to 1 msec accuracy, are stored on the spacecraft solid-state tape recorder along with housekeeping data. At the end of each orbital night, detector high voltages are ramped back to idle levels to protect them from damage and the spacecraft returns to solar array pointed attitude. Up to four times per 24 hour day the solid state recorder is dumped via the X-band transmitter to ground stations in Hawaii or Perth, Australia.

The GALEX data analysis pipeline operated at the Caltech Science Operations Center receives the time-tagged photon lists, instrument/spacecraft housekeeping and satellite aspect information. From these data sets, the pipeline reconstructs the aspect vs. time and generates images, spectra and source catalogs. The first pipeline module corrects the photon positions for detector and optical distortions and calculates an optimal aspect solution based on the time-tagged photon data and star catalogs. A photometric module accumulates the photons into count and intensity maps and extracts sources using a modified version of SExtractor (?). A spectroscopic module uses image source catalog inputs to extract spectra of these sources from the multiple slitless grism observations.

A summary of on-orbit performance is given in Table 1, and full details on the on-orbit performance are given by Morrissey et al. (2004), in the following paper.

2.3. Survey Design

Night sky backgrounds in the GALEX bands are low: the FUV[NUV] is dominated by diffuse galactic light[zodiacal light], with typical levels 27.5[26.5] mag arcsec⁻² corresponding to 3[30] photon/PSF in one eclipse. Surveys become background limited at $m_{AB} \sim 23.5$. Targets are constrained by the current bright star limit for the detectors (5 kcps) which makes 50% of the sky inaccessible. This limit will be raised to 50 kcps shortly.

All-sky Imaging Survey (AIS). The goal of the AIS is to survey the entire sky subject to a sensitivity of

TABLE 2
SURVEY SUMMARY

Survey	Area [deg ²]	Expos [ksec]	m_{AB}	#Gals (est.)	Volume [Gpc ³]	$< z >$
All-Sky Imag. (AIS)	40,000	0.1	20.5	10 ⁷	1	0.1
Medium Imag. (MIS)	1000	1.5	23	10 ^{6.5}	1	0.6
Deep Imaging (DIS)	80	30	25	10 ⁷	1.0	0.85
Ultra-Deep Imag.(UDIS)	1	200	26	10 ^{5.5}	0.05	0.9
Nearby Galaxies (NGS)	—	0.5	27.5 ^a	200	—	—
Wide Spectro.(WSS)	80	30	20	10 ⁴⁻⁵	0.03	0.15
Medium Spectro. (MSS)	8	300	21.5 ^b	10 ⁴	0.03	0.3
			23.3 ^c	10 ⁵	0.03	0.5
Deep Spectro. (DSS)	2	2000	22.5 ^b	10 ⁴	0.05	0.5
		2000	24.3 ^c	10 ⁵		0.9

^amag. sq. arcsec ^b R=100; ^cR=20

$m_{AB} \simeq 20.5$, comparable to the POSS II ($m_{AB}=21$) and SDSS spectroscopic ($m_{AB}=17.6$) limits. Several hundred to 1000 objects are in each 1 deg² field. The AIS is performed in roughly ten 100-second pointed exposures per eclipse (~ 10 deg² per eclipse).

Medium Imaging Survey (MIS). The MIS covers 1000 deg², with extensive overlap of the Sloan Digital Sky Survey. MIS exposures are a single eclipse, typically 1500 seconds, with sensitivity $m_{AB} \simeq 23$, net several thousand objects, and are well-matched to SDSS photometric limits.

Deep Imaging Survey (DIS). The DIS consists of 20 orbit (30 ksec, $m_{AB} \simeq 25$) exposures, over 80 deg², located in regions where major multiwavelength efforts are already underway. DIS regions have low extinction, low zodiacal and diffuse galactic backgrounds, contiguous pointings of 10 deg² to obtain large cosmic volumes, and minimal bright stars.

Nearby Galaxies Survey (NGS). The NGS targets well-resolved nearby galaxies for 1-2 eclipses. Surface brightness limits are $m_{AB} \sim 27.5$ arcsec⁻², or a star formation rate of $10^{-3} M_{\odot} \text{ yr}^{-1} \text{ kpc}^{-2}$. The 200 targets are a diverse selection of galaxy types and environments, and include most galaxies from the Spitzer IR Nearby Galaxy Survey (SINGS) along with extensive ground-based coverage. Figure 2 shows the NGS observation of the M81/M82 system.

Spectroscopic Surveys. The suite of spectroscopic surveys includes (1) the Wide-field Spectroscopic Survey (WSS), which covers the full 80 deg² DIS footprint with comparable exposure time (30 ksec), and reaches $m_{AB} \sim 20$ for S/N ~ 10 spectra; (2) the Medium Spectroscopic Survey (MSS), which covers the high priority central field in each DIS survey region (total 8 deg²) to $m_{AB}=21.5-23$, using 300 ksec exposures; and (3) Deep Spectroscopic Survey (DSS) covering 2 deg² with 1000 eclipses, to a depth of $m_{AB}=23-24$.

3. EARLY RESULTS

In this dedicated Astrophysical Journal Letters issue, we describe a selection of early results obtained from the GALEX surveys. In this introductory letter, we give examples of data from the various surveys and highlight some of the early results described in more detail in this issue.

3.1. Star Formation in Diverse Contexts

GALEX observations demonstrate that rest UV emission traces star formation in a wide variety of contexts, environments and modalities. In nearby quiescent disk galaxies (M101, M51, M33) GALEX observations provide the ages, luminosities, masses, and extinction of star formation complexes. These show that the cluster age distribution is consistent with a constant star formation rate over the last 10⁹ Myrs (Bianchi et al. 2004).

GALEX has discovered extended UV emission far outside (2-4 times) the optical disk of a number of nearby spiral galaxies, including M83 and NGC628. Star formation appears to be proceeding at gas surface densities below the typical galactic threshold, and the complexes formed appear to have lower luminosity, mass, and younger ages than those in the inner disk (Thilker et al. 2004).

In the Antennae merger system, recent star formation has occurred in the disk, tails and Tidal Dwarf Galaxy on timescales less than the 300 Myr dynamical time, implying that star formation is triggered in the tidal streams after gas leaves the galaxy (Hibbard et al. 2004). GALEX has detected UV emission in extended tidal tails of a number of other interacting galaxies (Neff et al. 2004a; Xu et al. 2004b) showing ages less than interaction times, suggesting that interaction-induced star formation in tidal gas streams may be a common phenomenon. Star formation triggered in an HI 50 kpc from Centaurus A (Neff et al. 2004b) is easily detected in the UV. All of these phenomena are likely to be more common at high redshift.

3.2. Star Formation History

Large area, unbiased, multiwavelength surveys support a robust statistical study of the fundamental properties of galaxies. GALEX provides an unprecedented measurement of the star formation rate. When combined with rest optical/near IR, the key parameter of star formation rate per unit stellar mass (specific star formation rate), which is closely related to the current star formation rate with respect to the average, can be determined over a wide dynamic range.

GALEX combined with the Sloan Digital Sky Survey forms a powerful dataset. GALEX-SDSS colors provide preliminary source classification and characterization (Seibert et al. 2004a), separating main sequence, post-main-sequence, and binary stars, QSOs, and galaxies. GALEX/SDSS photometry provide excellent measurement of the ratio of current to average star formation rates (the b -parameter) and important constraints on starburst history in the local universe (Salim et al. 2004).

In the local universe UV luminosities follow a Schechter function with $L_* = 2 \times 10^9 L_{\odot}$ (Wyder et al. 2004), with measurably different parameters for red and blue subsamples and evidence for evolution (Treyer et al. 2004). The luminosities functions and resulting luminosity densities are significantly fainter than those obtained by FOCA. GALEX on-orbit calibration shows excellent agreement with the ground calibration (Morrissey et al. 2004), so we attribute this discrepancy to an overestimate of fluxes at faint magnitudes by FOCA. GALEX number count distributions fall below those of FOCA, show some evidence for evolution, and show some flattening at faint magnitudes due to a combination of blending, confusion, and faint wing overlap (Xu et al. 2004a).

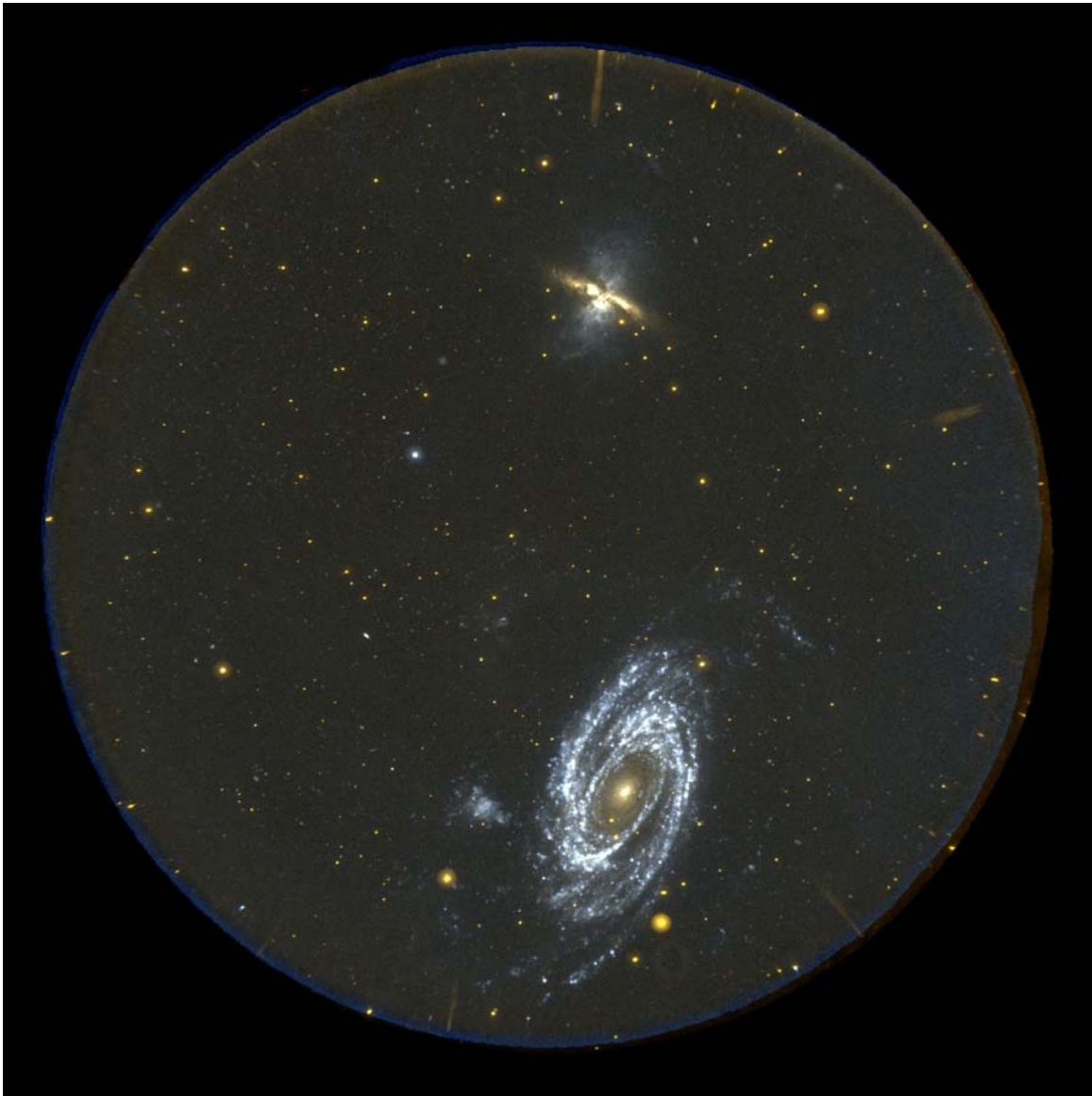


FIG. 2.— In Figure 2, we show the GALEX NGS observation of the M81-M82 system. This figure illustrates how a single GALEX image may be used to study many different aspects of galaxy evolution: spiral structure, stellar populations, extinction (M81), interaction-induced starbursts and resulting galactic outflows (M82); star formation in dwarf galaxies (Ho IX), between galaxies and in tidal streams; the UV background; and large scale structure.

GALEX-DIS data, combined with the VLT/VIMOS redshift survey, has provided the first GALEX measurements of the evolution of the UV luminosity function and density (Arnouts et al. 2004). Significant evolution is found, consistent with $\sim (1+z)^2$. When corrected for extinction using the Kong, Charlot, Brinchmann, & Fall (2004) prescription, this provides the first GALEX measurements of cosmic SFR history over $0 < z < 1.2$ (Schiminovich et al. 2004). When combined with consistent analysis of deep optical data from HDF-N (Arnouts et al. 2004; Schiminovich et al. 2004), the results suggest a monotonic decline in the star formation rate density since $z=3$, rather than a peak at $z \sim 1-1.5$.

The GALEX AIS/MIS-SDSS DR1 matched datasets have yielded the discovery of Luminous UV Galaxies (LUGs), galaxies with UV luminosities and properties comparable to Lyman Break Galaxies, in the local uni-

verse (Heckman et al. 2004). LUGs have 500 times lower space density than LBGs, but their number rises sharply toward higher redshift (Schiminovich et al. 2004). LUGs may provide an excellent opportunity to study low redshift analogs to young, high redshift, star-forming galaxies.

3.3. Dust Extinction

UV extinction by dust remains the principle obstacle in converting UV luminosity directly to SFR. In individual galaxies (M83 and M101), we show that extinction is strongly declining function of radius and may contain a significant diffuse, interarm component (Popescu et al. 2004; Boissier et al. 2004).

With IRAS data, we have begun to characterize the properties of FUV and Far-IR selected galaxy samples in the local universe. As expected, flux-limited UV and

Far-IR selected samples yield different projections of the bivariate UV/Far-IR luminosity function and distinct UV/Far-IR ratios (Buat et al. 2004). However, virtually all star-forming galaxies detected in local Far-IR-selected samples are also detected by GALEX. The SFR luminosity function places a fundamental constraint on cosmological models. The bivariate UV/FIR luminosity function, obtained from combined UV and FIR selected samples, shows a bimodal behavior: L_{FUV} tracks L_{FIR} for $L_{TOT} < 3 \times 10^9 L_{\odot}$, and L_{FUV} saturates for higher total luminosities. The total SFR function is log-normal function over four decades of luminosity (Martin et al. 2004b).

Starburst galaxies in the local universe display a well-known relationship between UV slope (β) and Far-IR-to-UV luminosity ratio (IRX). Early results from GALEX indicate that 1) normal and quiescent star forming galaxies fall below the canonical IRX- β relation for starbursts, perhaps due to starburst age (Kong, Charlot, Brinchmann, & Fall 2004); and 2) the difference between starbursts and ULIRGs within IRX- β space is not as distinct as previously suggested, which is consistent with our observation that galaxies span a continuum in the bivariate UV/Far-IR luminosity function.

3.4. UV from Stars, Gas, Dust, and AGN

In addition to recent star formation, UV traces dust through scattering and absorption, gas by emission lines and two-photon continuum, hot evolved stars and late-type stellar chromospheres, degenerate binaries, and QSOs. While the average elliptical galaxy show evidence for residual star formation at the 1-2% level (Yi et al. 2004), quiescent ellipticals (notably in rich clusters) exhibit the well known UV excess but without the previously claimed correlation with metallicity index (Rich

et al. 2004). The M82 outflow, prominent in Figure 2, is injecting abundant dust into the IGM, which reflects UV from the obscured starburst (Hoopes et al. 2004). In our own galaxy, the remarkable Criss-Cross nebula shines brightly in two-photon continuum from a moderate velocity shock (Seibert et al. 2004c). As the AIS progresses, the number of QSOs suitable for measurements of HeII reionization are increasing (Tytler et al. 2004).

4. GALEX DATA LEGACY

GALEX Early Release Data was made available in December, 2003. The first major data release, GDR1, will occur on October 1, 2004, coincident with the start of the GALEX Guest Investigator Program. All GALEX data are served by the StScI MAST Archive. While we cannot predict the applications to which the GALEX data will be applied in the future, we can anticipate that the impacts of the first comprehensive UV Sky Survey will be broad and lasting.

GALEX (Galaxy Evolution Explorer) is a NASA Small Explorer, launched in April 2003. We gratefully acknowledge NASA's support for construction, operation, and science analysis for the GALEX mission, developed in corporation with the Centre National d'Etudes Spatiales of France and the Korean Ministry of Science and Technology. The grating, window, and aspheric corrector were supplied by France. We acknowledge the dedicated team of engineers, technicians, and administrative staff from JPL/Caltech, Orbital Sciences Corporation, University of California, Berkeley, Laboratoire Astrophysique Marseille, and the other institutions who made this mission possible.

REFERENCES

- Adelberger, K. L. & Steidel, C. C. 2000, ApJ, 544, 218
 Arnouts, S. et al. 2004, ApJ, this issue.
 Bennett, C. L. et al. 2003, ApJS, 583, 1
 Bianchi, L. et al. 2004, ApJ, this issue.
 Boissier, S. et al. 2004, ApJ, this issue.
 Boksenberg, A., et al. 1973, MNRAS, 163, 291
 Bowyer, S., Sasseen, T. P., Lampton, M., & Wu, X. 1993, ApJ, 415, 875
 de Bernardis, P. et al. 2000, Nature, 404, 955
 Buat, V. et al. 2004, ApJ, this issue.
 Carruthers, G. R. 1973, Appl. Opt. 12, 2501.
 Code, A. D., Houck, T. E., McNall, J. F., Bless, R. C., & Lillie, C. F. 1970, ApJ, 161, 377
 Fall, S. M., Charlot, S., & Pei, Y. C. 1996, ApJ, 464, L43
 Dickinson, M., Papovich, C., Ferguson, H. C., & Budavári, T. 2003, ApJ, 587, 25
 Giavalisco, M., et al. 2004, ApJ, 600, L93
 Gil de Paz, A. et al. 2004, ApJ, this issue.
 Heckman, T. et al. 2004, ApJ, this issue.
 Henize, K. G., Wray, J. D., Parsons, S. B., Benedict, G. F., Bruhweiler, F. C., Rybski, P. M., & Ocallaghan, F. G. 1975, ApJ, 199, L119
 Hibbard, J. et al. 2004, ApJ, this issue.
 Hoopes, C. et al. 2004, ApJ, this issue.
 Kennicutt, R. C. 1989, ApJ, 344, 685
 Kondo, Y., ed. in chief, "Exploring the Universe with the IUE Satellite", 1987, D. Reidel: Dordrecht.
 Kong, X., Charlot, S., Brinchmann, J., & Fall, S. M. 2004, MNRAS, 349, 769
 Lee, Y.-W. et al. 2004, ApJ, this issue.
 Lilly, S. J., Le Fevre, O., Hammer, F., & Crampton, D. 1996, ApJ, 460, L1
 Madau, P., Ferguson, H. C., Dickinson, M. E., Giavalisco, M., Steidel, C. C., & Fruchter, A. 1996, MNRAS, 283, 1388
 Martin, D. C. et al. 2004, ApJ, this issue.
 Martin, C. et al. 2003, Proc. SPIE, "Future EUV/UV and Visible Space Astrophysics Missions and Instrumentation", vol. 4854, p. 336.
 Meurer, G. R., Heckman, T. M., & Calzetti, D. 1999, ApJ, 521, 64
 Milliard, B., Laget, M., & Donas, J. 1992, IAU Commission on Instruments, 2, 49
 Morrissey, P., et al., 2004., this issue.
 Neff, S. et al. 2004, ApJ, this issue.
 Neff, S. et al. 2004, ApJ, this issue.
 Popescu, C. et al. 2004, ApJ, this issue.
 Rey, S.-C. et al. 2004, ApJ, this issue.
 Rich, R. M. et al. 2004, ApJ, this issue.
 Salim, S. et al. 2004, ApJ, this issue.
 Schiminovich, D. et al. 2004, ApJ, this issue.
 Seibert, M. et al. 2004, ApJ, this issue.
 Seibert, M. et al. 2004, ApJ, this issue.
 Seibert, M. et al. 2004, ApJ, this issue.
 Stecher, T. P., et al. 1997, PASP, 109, 584
 Steidel, C. C., Giavalisco, M., Pettini, M., Dickinson, M., & Adelberger, K. L. 1996, ApJ, 462, L17
 Thilker, D. et al. 2004, ApJ, this issue.
 Tinsley, B. M. 1968, ApJ, 151, 547
 Treyer, M. et al. 2004, ApJ, this issue.
 Treyer, M. A., Ellis, R. S., Milliard, B., Donas, J., & Bridges, T. J. 1998, MNRAS, 300, 303
 Tytler, D. et al. 2004, "STIS Spectroscopy of HeII in the IGM", HST Cycle 13 Proposal, accepted.
 van Duinen, R. J., Aalders, J. W. G., Wesselius, P. R., Wildeman, K. J., Wu, C. C., Luinge, W., & Snel, D. 1975, A&A, 39, 159

Wyder, T. et al. 2004, ApJ, this issue.
Xu, C. K. et al. 2004, ApJ, this issue.
Xu, C. K. et al. 2004, ApJ, this issue.

Yi, S. Y. et al. 2004, ApJ, this issue.